Dipolar localization of quantized spin-wave modes in thin rectangular magnetic elements

K. Y. Guslienko,[1] R. W. Chantrell,[1] and A. N. Slavin[2]
[1]*Seagate Research, Pittsburgh, Pennsylvania 15222, USA*
[2]*Department of Physics, Oakland University, Rochester, Michigan 48309, USA*
(Received 2 April 2003; published 30 July 2003)

Dipole-exchange spectrum of quantized spin wave modes of a tangentially magnetized rectangular thin-film magnetic element is calculated using the method of tensorial Green's functions. The strong inhomogeneity of the internal bias magnetic field along the magnetization direction leads to the localization of spin wave modes either at the edges (exchange localization) or at the center (dipolar localization) of the element. The mode intensity distributions along the other in-plane direction are determined by the dipolar boundary conditions and have the usual cosinusoidal form. The approximate theory developed in the paper gives a quantitative description of the resonance fields and qualitative description of the spatial distributions of quantized spin wave modes in a thin square permalloy element (in plane sizes $50\times 50\ \mu m^2$, thickness 0.1 μm) recently observed by space-resolved Kerr spectroscopy. The theory shows also that the mode localization in this case (in the element center) is of the dipolar nature.

DOI: 10.1103/PhysRevB.68.024422 PACS number(s): 75.30.Ds, 75.40.Gb

INTRODUCTION

The experiments performed on patterned magnetic films with the patterns in the form of micrometer-sized rectangular magnetic stripes or dots have demonstrated that the spin wave (SW) spectrum of these patterned films is quantized.[1–5] The observed geometrical quantization is a direct consequence of the boundary conditions at the lateral edges of the magnetic elements forming a pattern. Similar results, i.e., the geometrical quantization of the SW spectrum, were obtained on the arrays of submicrometer-sized tangentially magnetized elliptical[6] and cylindrical dots[4] (see also Ref. 7, and references therein).

The calculation of the eigenfrequencies of quantized SW modes in small magnetic elements (or resonators) is nontrivial and important for several reasons. First of all, the spin wave mode quantization in small magnetic elements is fundamentally interesting due to the nonellipsoidal shape of most of these elements. The internal bias magnetic field in nonellipsoidal magnetic resonators is inhomogeneous, which leads to the coordinate-dependent variation of the wave numbers of resonant spin wave modes and to the appearance of ''turning points'' and effective ''potential wells'' for spin waves inside the magnetic elements.[8–11]

On the other hand, there is a practical necessity to calculate the eigenfrequencies of spin wave modes of small (submicron size) magnetic elements. In order to avoid unwanted ''ringing'' in the re-magnetization process of a pattern element, the duration of the ''writing'' pulse should be equal to the half period of the lowest spin-wave eigenmode of the element.[12,13] Also, one of the most important limitations in operation of magnetic sensors and recording heads (that, essentially, are small magnetic elements) working in the microwave frequency range is the magnetic noise[14,15] that has spectral maxima near the frequencies of SW eigenmodes in these elements.

The experiments,[2–4] where the quantization effect in patterned metal films was clearly demonstrated and understood, were performed on the pattern of long permalloy stripes with rectangular cross-section magnetized *longitudinally* (along the stripe axis).[1,2,4] In the case of a long stripe only one component (along the stripe width) of the SW wave vector is quantized, so the quantization process is one dimensional and relatively simple. Also, in that case the internal bias magnetic field in the stripe is homogeneous and equal to the external bias field, while the weak inhomogeneity of the *dynamic* demagnetizing field leads to the effective ''pinning'' of the dynamic magnetization at the lateral edges of the stripe that can de described by effective dipolar boundary conditions.[16] Thus, the lowest quantized spin wave modes in this case are essentially a result of quantization of the Damon-Eshbach surface magnetostatic mode[17] under the boundary conditions.[16]

Further experiments[10,11] performed on *transversely* (perpendicular to the stripe axis) magnetized permalloy stripes (width 1 μm, thickness 0.03 μm) have demonstrated that quantization of dynamic magnetization in this case is dramatically different from the case of longitudinal magnetization. First of all, in the transverse case the waves from which the quantized spin wave mode is formed are *dipole-exchange backward volume* spin waves having wave vectors parallel to the bias magnetic field. At the small wave vector magnitudes (or/and in the nonexchange limit) the frequency of these waves decreases with the increase of their wave vector.[16] Second, the internal bias field along the stripe width is strongly inhomogeneous, and the quantized spin wave mode of a fixed frequency is composed of many plane waves having different magnitudes of the wave vector. Thus, in transversely magnetized narrow permalloy stripes the lowest quantized spin wave modes turn out to be of mostly exchange nature and are localized in ''potential wells'' formed by the strongly inhomogeneous bias magnetic field near the lateral edges of the stripe.[10,11]

Recently, the quantization of SW modes has been observed in tangentially magnetized and relatively large square permalloy film elements (in plane sizes $50\times 50\ \mu m^2$, thickness 0.1 μm) by means of space-resolved Kerr spectroscopy[18] and by inductive FMR spectroscopy.[19] In contrast with previous studies of rectangular magnetic elements,[1,3,19] where the quantized spin wave spectra were

observed, the experiment[18] gave not only the resonance fields (or frequencies), but also the spatial distributions of variable magnetization in the observed quantized spin wave modes. Thus, it is very interesting to compare the experimental results[18] with the theory.

The quantization of spin wave modes in a thin rectangular magnetic element (or dot) having *two* finite in-plane dimensions is much more complicated than the one-dimensional spin wave quantization in the long stripes.[2,3,5,10,11] In a tangentially magnetized rectangular dot the quantization is two-dimensional, and the cases of longitudinal and transverse magnetization occur simultaneously for two perpendicular components of the resonant in-plane wave vector.

The goal of this paper is to analyze theoretically the two-dimensional problem of spin wave quantization in a nonellipsoidal rectangular magnetic element and to derive an approximate analytical expression for the dipole-exchange spectrum of the discrete spin wave modes of this element, that takes into account the boundary conditions at the element lateral edges, the inhomogeneity of the bias magnetic field inside the element, and describes, in particular, the results of the experiment.[18]

CALCULATION METHOD

Our theoretical approach is based on the tensorial Green's functions formalism for infinite in-plane magnetic films,[20] which takes into account both dipole-dipole and exchange contributions to the SW spectra. Later this formalism was modified in Ref. 21 to describe finite in-plane sizes of a thin magnetic element. In the limit of a very thin magnetic element similar formalism as used in Ref. 1 was derived on the basis of the Sparks variational approach.[22]

In the framework of this formalism, Maxwell equations in the magnetostatic limit are solved to find a tensorial Green's function that defines a nonlocal integral relation between the dynamic demagnetizing field and the variable magnetization for the particular geometry of the magnetic element. Then this integral relation is used in the Landau-Lifshits equation of motion for the variable magnetization where the differential operator of the exchange interaction is included. This equation of motion is eventually reduced to a linear integrodifferential equation for the variable magnetization that is solved by expanding the variable magnetization in a series of complete orthogonal eigenfunctions (*approximate* spin wave modes), that satisfy the boundary conditions for the variable magnetization existing at the edges of the magnetic element (see Refs. 20, 21 for details). If we neglect the interaction between these approximate spin wave modes, it is possible to derive a simple approximate diagonal analytical expression for the dipole-exchange spin wave spectrum of a finite-size magnetic element.

Below we consider thin rectangular magnetic elements with typical in-plane sizes $\sim 1-10\ \mu$m and thickness 20–100 nm. We denote the element length l, width w, thickness L, and let the static magnetization lie in the xy plane, so that the $0z$ axis is directed along the element height and the origin of the Cartesian coordinate system is at the center of the element bottom surface (see Fig. 1). The homogeneous external magnetic field **H** is directed along the Oy axis in the element plane. We assume that the static magnetization $\mathbf{M}_s(\mathbf{r})$ (where $\mathbf{r}=x\mathbf{e}_x+y\mathbf{e}_y+z\mathbf{e}_z$, and $\mathbf{e}_x$, $\mathbf{e}_y$, and $\mathbf{e}_z$ are the unit vectors along the axes x, y, and z correspondingly) of the element is uniform or nearly uniform, except at the element edges. We consider the case of a flat rectangular particle ($L/l \ll 1, L/w \ll 1$), and assume uniform distribution of microwave magnetization along the Oz axis.

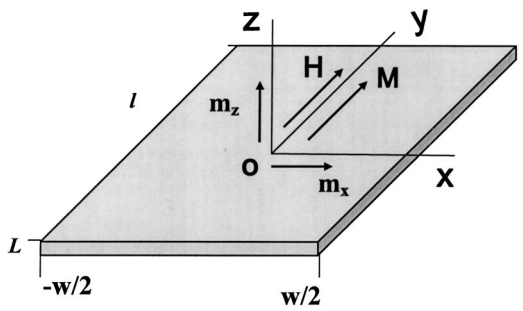

FIG. 1. Geometry of the problem (thin rectangular element) and the system of coordinates. Bias field H and static magnetization are in the element plane.

The theory of the dipole-exchange spin wave spectrum in a magnetic film having finite thickness L and infinite in-plane sizes has been developed in Ref. 20, where an approximate explicit expression for the dipole-exchange SW dispersion equation $\omega=f(k_x,k_y,k_z)$ (note change of F to f) was obtained [see Eq. (45) in Ref. 20]. To take into account the finite sizes of the rectangular magnetic element it is possible (in a first approximation for a thin element) to introduce quantized values for the SW wave vector **K** components (k_x,k_y,k_z)

$$K^2=k_z^2+k_\parallel^2=(p\pi/L)^2+k_{mx}^2+k_{ny}^2, \tag{1a}$$

where p, m, $n=0,1,2,\ldots$.

We assume, that at the plane surfaces of the magnetic element the spins are unpinned, so that the lowest thickness SW mode is uniform ($p=0$). Thus, below we shall take into account only the quantization of the in-plane (k_x,k_y) components of the wave vector **K** of the spin wave mode

$$K^2 \to \kappa_{mn}^2=k_{mx}^2+k_{ny}^2. \tag{1b}$$

The demagnetizing field $\mathbf{H}_d(\mathbf{r})$ obtained from the solution of the Maxwell equations in the magnetostatic limit is nonuniform for the nonellipsoidal elements (even for uniform $\mathbf{M}_s$), and has three components. If the variable magnetization does not depend on z, then we can average the components of the field $\mathbf{H}_d(\mathbf{r})$ over z. Since the component $H_d^z(z)$ is an odd function with respect to the dot center $z=L/2$ it vanishes after averaging. We also neglect the term $(\gamma H_d^x/\omega)^2 \sim (L/w)^2 \ll 1$ (where ω is the SW mode frequency and γ is the gyromagnetic ratio) in the equation of motion for the variable dot magnetization **m**. Thus, only one component (along the magnetization direction y) $H_d^y(x,y)=\langle H_d^y(\mathbf{r})\rangle_z$, of the demagnetizing field remains and it depends only on the in-plane coordinates x, y for all SW modes. The nonuniform demagnetizing field $H_d^y(\rho)=-4\pi N_{yy}(\rho)M_s$, (where

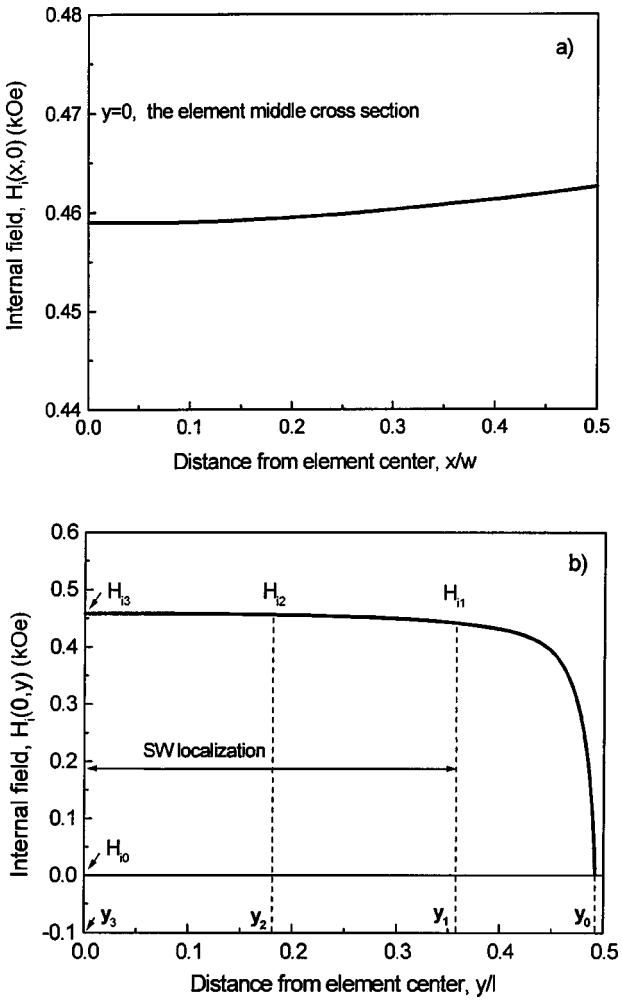

FIG. 2. 2D internal field $H_i(x,y)$ distribution calculated according to Ref. 23 for the first SW mode: (a) dependence on x; (b) dependence on y (along bias field).

$\rho = x\mathbf{e}_x + y\mathbf{e}_y$) can be evaluated using the effective coordinate-dependent demagnetizing factor $N_{yy}(\rho)$ derived in Refs. 23, 24 [see Eq. (16) in Ref. 23]. Therefore, the nonuniform internal bias magnetic field inside the rectangular magnetic element can be expressed in terms of the uniform external bias field H and saturation magnetization M_s as

$$H_i(\rho) = H - 4\pi M_s N_{yy}(\rho). \tag{2}$$

Since the internal bias field (2) is coordinate dependent, the influence of the bias field inhomogeneity will be different for different mode profiles and we, basically, need to introduce a different averaged internal bias field for different SW modes.

The dependence of the internal bias field $H_i(x)$ on the coordinate x calculated at the center ($y=0$) of the square permalloy element used in the experiments[18] for the value of the homogeneous *external* bias magnetic field $H(\mathrm{P1})$, corresponding to the observation of the lowest quantized spin wave mode in Ref. 18 (mode P1 in the notation of Ref. 18) is shown in Fig. 2(a). This curve was calculated using Eq. (2) and the equations from Ref. 23. It is clear from Fig. 2(a) that the curve $H_i(x)$ is smooth and the field nonuniformity is weak. This situation is similar to the case of a longitudinally magnetized magnetic stripe.[16] At the same time, in the other in-plane direction Oy (along the static magnetization $\mathbf{M}_s$) there is a strong coordinate dependence of the internal bias magnetic field $H_i(y)$ even at the center of the magnetic element ($x=0$) [see Fig. 2(b)]. This situation is similar to the case of a transversely magnetized long magnetic stripe.[10] The values H_{i0}, H_{i1}, H_{i2}, H_{i3} of the internal bias field marked in Fig. 2(b) correspond to four different locations in the element along the axis y (y_0, y_1, y_2, y_3) and will be used later.

In the analysis below we shall make the following simplifying assumption. We shall assume that in a rectangular magnetic element the quantization of the x component k_x of the in-plane wave vector takes place as in the longitudinally magnetized long stripe,[16] the quantization of the y component k_y of the wave vector takes place as in the transversely magnetized long stripe,[10] and the two-dimensional approximate spin wave eigenfunctions of the rectangular magnetic elements are products of one-dimensional spin wave eigenfunctions obtained in the cases of longitudinally and transversely magnetized magnetic stripes, correspondingly.

Then, the quantization condition for the x-component of the wave vector will have the form[16]

$$k_{mx} = \frac{(m+1)\pi}{w}\left[1 - \frac{2}{d(p)}\right], \quad m = 0,1,2,..., \tag{3}$$

where the value of the parameter of the effective dipolar "pinning" at the lateral edges of the rectangular magnetic element depends only on the ratio $p = L/w \ll 1$ of the element thickness L to its width w, and is given by the expression $d(p) = 2\pi/[p(1-2\ln p)]$.[16] The quantization condition (3) can be rewritten as $k_{mx} = (m+1)\pi/w_{\mathrm{eff}}$, where the effective width of the stripe $w_{\mathrm{eff}} = w[d/(d-2)]$ is always slightly larger than the real width w. The distribution of variable magnetization in symmetric spin wave modes obtained from the quantization condition (3) has a simple cosinusoidal form[16]

$$m_{mx}(x) = A_{mx}\cos(k_{mx}x). \tag{4}$$

The scheme of SW mode quantization along the direction of the bias magnetic field Oy is more complicated due to the inhomogeneity of the internal bias field along this direction [see Fig. 2(b)]. This scheme is schematically illustrated by Fig. 3(a) where the dipole-exchange dispersion curves $\omega_{sw}(k_y)$ for spin waves propagating along the direction of the bias magnetic field in an infinite magnetic film are shown for two different values of the bias magnetic field corresponding to the values H_{i0} and H_{i3} marked in Fig. 2(b). These curves were calculated using Eq. (4) from Ref. 25 [or Eq. (45) from Ref. 20]. The horizontal broken line in Fig. 3(a) shows the frequency of the signal $\omega_0/2\pi = 7.04$ GHz used in the experiment,[18] that is the resonance frequency of the lowest SW mode in the square magnetic element when the external bias field is equal to the lowest spin wave mode resonance field $H_e(\mathrm{P1})$ (see Fig. 2 in Ref. 18). The vertical broken line in Fig. 3(a) shows the maximum value of the SW

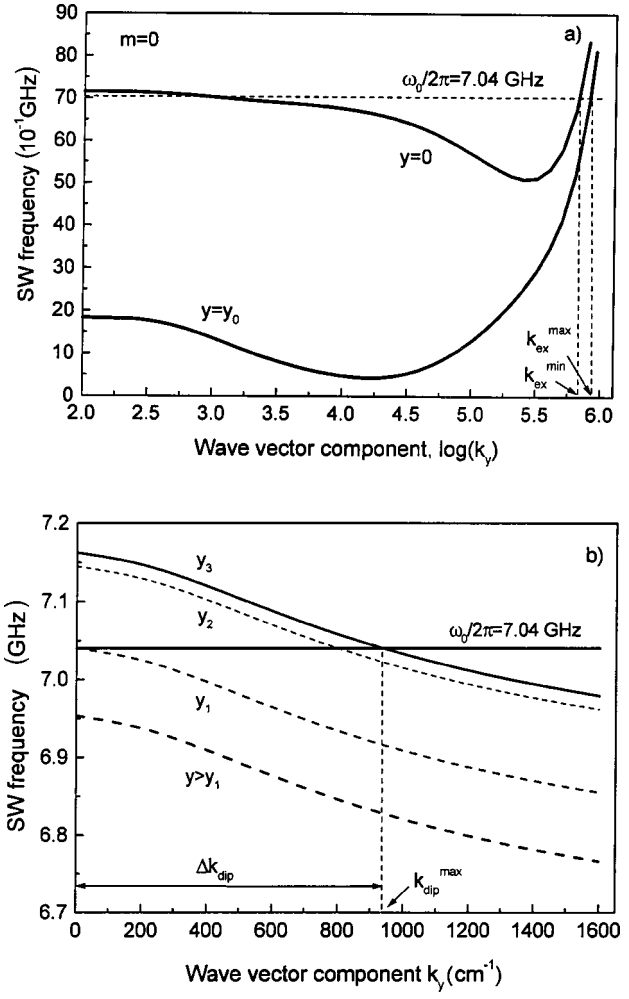

FIG. 3. Dependence of the SW frequency on the wave-vector component along bias field k_y (in cm^{-1}) for the lowest transverse mode $m=0$ (the transverse wave vector component is $k_{mx}=\pi/w$). The values of y_i as in Fig. 2(b). (a) The SW dispersion curve in the dipole-exchange region, (b) the dipolar part of the SW dispersion relation (small $k_y \sim 10^3\ \mathrm{cm}^{-1}$), $y=0$—solid line and $y=y_m$ (the last point of the frequency crossing)—dashed line. The interval of the dipolar wave vectors marked as Δk_{dip}.

wave vector component $k_y^{\max} \approx 2\pi/W_t \approx 2\times 10^4\ \mathrm{cm}^{-1}$ that can be effectively excited by the coplanar microwave transducer (width $W_t = 3\ \mu\mathrm{m}$) used in the experiments.[18]

It is clear from Fig. 3(a) that quantized spin wave modes (standing along the axis Oy and resonant at the frequency ω_0), are composed of dipole-exchange backward volume waves having different values of k_y. In Fig. 3(a) dipole-exchange SW dispersion curves cross the line $\omega_0/2\pi = 7.04$ GHz in two wave-number regions: in the ''dipolar'' region where the wave frequency decreases with the increase of k_y and the ''exchange'' region, where the wave frequency increases with the increase of k_y. Figure 3(b) shows the ''dipolar'' region in a larger scale in different points along Oy axis.

In principle, quantized SW modes could be formed in any of these two wave-number regions. Whether the quantized SW mode is really formed depends on the fulfillment of the

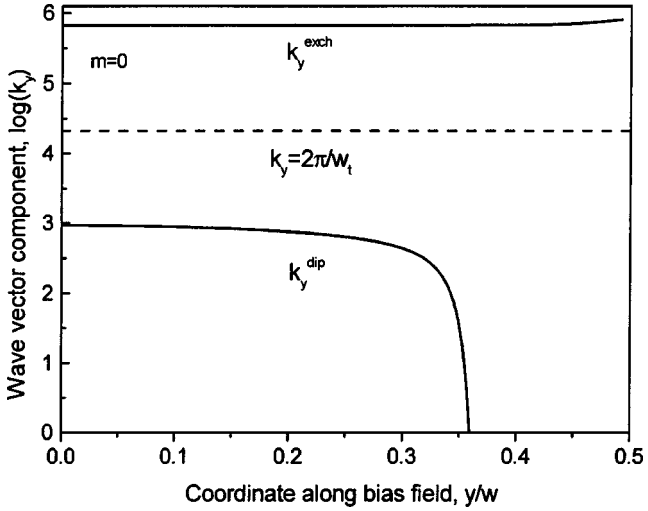

FIG. 4. The SW wave vector component k_y (in cm^{-1}) along the bias field (Oy) in the rectangular element as a function of y. The two branches k_y^{exch} and k_y^{dip} correspond to crossing of spin-wave dispersion relation given in Fig. 3(a) with the experimental frequency $\omega_0/2\pi = 7.04$ GHz (Ref. 18) for different values of the coordinate y.

integral quantization condition, similar to the quantization condition in the quasiclassical case in quantum mechanics (see Refs. 8–11, and references therein):

$$\oint k(y)\,dy = 2(n+1)\pi,$$

where the integral is taken over the closed path inside the classically allowed region between the ''turning'' points, i.e., inside the region where the wave number has *real* values. This leads to the following integral quantization condition for the k_y component of the SW wave vector parallel to the in-plane bias magnetic field:

$$\int_{y'}^{y''} k_y(y,\omega_0,H_e)\,dy = (n+1)\pi = \tilde{k}_{ny} l, \quad n=0,1,2,\ldots, \tag{5}$$

where y' and y'' are the ''turning points'' between which the equation $\omega_{sw}(k_y)=\omega_0$ has a real solution for k_y, and $\tilde{k}_{ny} = (n+1)\pi/l$ is the averaged value of the quantized wave vector component along the axis Oy.

The curves showing the dependences of k_y^{dip} and k_y^{ex} on the coordinate in the ''dipole'' and ''exchange'' regions of the spectrum Fig. 3(a) for the coordinate dependence of the internal bias field $H_y(y)$ given in Fig. 2(b) [and corresponding to the observation of the lowest $(n=0)$ quantized SW mode in the experiment[18]] are shown in Fig. 4. It is clear from these curves that in the dipolar region $k_y^{\mathrm{dip}}(y)$ decreases when y increases towards the edge of the magnetic element. At $y=y_1=0.359\,l$, where $k_y(y_m)=0$ the turning point is reached, and the dipolar SW mode could only exist between the points $y'=y_1$ and $y''=-y_1$. We note, that the value of y_1 is smaller than the critical point value $y_0/l=0.492$, where the internal bias field in the element vanishes $[H_i(y_0)=0]$, so the lowest SW mode is localized along the axis Oy near

the center of the magnetic element. This smooth localization is clearly seen for the lowest mode in the Kerr spectroscopy image presented in Ref. 18 (see the image P1 in Fig. 3 in Ref. 18).

It is also clear from these curves, that if the quantized SW mode would have been formed in the ''exchange'' region of the spectrum it would occupy all the available range of y values, where the internal bias field is positive $|y|<y_0$. Under the conditions of the experiment[18] the quantized mode in the ''exchange'' region cannot be excited (or observed) as the maximum value of the SW wave in-plane vector component that could be effectively excited by the coplanar microwave transducer used in Ref. 18 $k_y^{\max}\approx 2\pi/W_t\approx 2\times 10^4$ cm^{-1} is much smaller than the typical values of k_y^{ex} shown in the upper part of Fig. 4. The calculation of the quantization integral (5) in the dipolar region of the spectrum Figs. 3, 4 shows that for the external magnetic field H(P1), corresponding to the excitation of the lowest quantized SW mode in the experiment[18] the magnitude of the integral (5) is close to π, so the quantized mode with the quantization number $n=1$ along the axis Oy is excited.

We would like to note that the dipole-exchange SW quantization in the inhomogeneous bias field of a nonellipsoidal magnetic element is very sensitive to the actual geometrical sizes of the element and, as is usual in the cases when exchange interaction is important, no universal picture of this effect can be given. In particular, the considerations similar to the ones given above performed for the case of a transversely magnetized *narrow* (width $w=1\,\mu$m) magnetic stripe[10] led us to the conclusion, that the lowest quantized SW mode in the stripe is formed in the ''exchange'' region of the spectrum and is localized in narrow regions near the lateral edges of the stripe.[10] The formation of a quantized SW mode in the ''dipolar'' region in the spectrum is not possible in such a narrow stripe, as the quantization condition (5) cannot be satisfied in the ''dipolar'' region, where the values of $k_y^{\rm dip}$ are relatively low. Later, this conclusion was supported by the space-resolved Kerr experiment[11] that directly demonstrated the localization of the lowest quantized SW mode near the lateral edges of the stripe.

In contrast with the case of quantization along the axis Ox, where the distributions of the variable magnetization in the quantized mode are easily calculated using Eq. (4), the profile of the quantized mode along the axis Oy is difficult to calculate analytically. Attempts to get these profiles numerically in the particular case of a very thin magnetic element were undertaken in Ref. 1. Using our prior assumption about the factorization of the eigenmodes of the rectangular magnetic element we shall write the expression for these approximate eigenmodes of the transverse (perpendicular to the saturation magnetization $\mathbf{M}_s$) variable magnetization in the magnetic element in the form

$$m_{mn}(\rho)=M_s\cos(k_{mx}x)\mu_n(y), \tag{6}$$

where $\mu_n(y)$ is the unknown distribution of quantized eigenmode along the coordinate y.

In general, to find the dipolar eigenfunction $\mu_n(y)$ an appropriate integral equation (similar to the dipolar integral equation discussed in Ref. 16) should be solved. However, we shall show below that the spectrum of SW eigenmodes in a thin ($L\ll w,\ l$) square magnetic element[18] can be calculated approximately without the exact knowledge of the function $\mu_n(y)$, simply assuming that $\mu_n(y)$ is a smooth function having maximum in the element center.

Expanding the variable magnetization in a Fourier series of two-dimensional approximate eigenfunctions (6) and using the standard formalism,[20,21] we obtain an approximate diagonal dipole-exchange dispersion equation for the quantized SW modes in a tangentially magnetized thin ($L\ll w,\ l$) magnetic element in the form similar to the form of the Herring-Kittel spin wave dispersion equation for the infinite ferromagnetic medium[26] and to the form of the approximate dipole-exchange dispersion equation for spin waves in a magnetic film[20] [see Eq. (45) in Ref. 20]

$$\omega_{mn}^2=(\omega_H^{mn}+\alpha\omega_M\kappa_{mn}^2)[\omega_H^{mn}+\alpha\omega_M\kappa_{mn}^2+\omega_M F_{mn}(\kappa_{mn})], \tag{7}$$

where $\omega_H=\gamma H$, $\omega_M=4\pi\gamma M_s$, α is the exchange constant, and κ_{mn} is defined by Eq. (1b). The frequency ω_H^{mn} proportional to the effective internal magnetic field for a SW mode with indices $(m,\ n)$ is defined by the formula [obtained from Eq. (2)]

$$\omega_H^{mn}=\omega_H-\omega_M N_{mn}, \tag{8}$$

and the effective demagnetization factor N_{mn} for the mode (m,n) is defined by the expression

$$N_{mn}=\frac{4}{wlM_s^2}\int d^2\rho m_{mn}^2(\rho)N_{yy}(\rho). \tag{9}$$

The quantity $F_{mn}(\kappa_{mn})$ plays the role of a quantized matrix element of the dipole-dipole interaction and has the form similar to the form of the analogous quantity defined by Eq. (4) in Ref. 20

$$F(\kappa_{mn})=1+P(\kappa_{mn})[1-P(\kappa_{mn})]\left(\frac{\omega_M}{\omega_H^{mn}+\alpha\omega_M\kappa_{mn}^2}\right)\left(\frac{k_{mx}^2}{\kappa_{mn}^2}\right)$$
$$-P(\kappa_{mn})\left(\frac{k_{ny}^2}{\kappa_{mn}^2}\right), \tag{10}$$

where

$$P(\kappa_{mn})=1-\frac{1-\exp(-\kappa_{mn}L)}{\kappa_{mn}L}. \tag{11}$$

We note that Eq. (8) is essentially the dispersion equation for spin waves in a tangentially magnetized magnetic film [see Eq. (45) in Ref. 20], where the in-plane components of the SW wave vector are quantized in accordance with the quantization conditions (3) and (5), that take into account the finite in-plane sizes of the magnetic element.

The second term in Eq. (10) describes the increase of the SW frequency with the increase of the magnitude of the component of the quantized wave vector that is perpendicular to the bias magnetic field (or well-known dispersion of the Damon-Eshbach magnetostatic surface wave[17]), while

TABLE I. Comparison of experimental (Ref. 18) and calculated resonance fields of square FeNi element. $l=w=50\ \mu$m, $L=104$ nm, $m=0$, 2, 4, 6, 8; $n=0$. $M_s=860$ G, $\gamma/2\pi=3.04$ GHz/kOe.

The SW mode number, (m,n)	(0,0)	(2,0)	(4,0)	(6,0)	(8,0)
Experimental resonance fields, Oe	469	392	324	261	196
Calculated $(m, 0)$–fields by Eq. (5), Oe	466	396	330	266	204

the last term in Eq. (10) describes the decrease of the SW frequency with the increase of the magnitude of the component of the quantized wave vector that is parallel to the bias magnetic field (or well-known dispersion of backward volume magnetostatic wave[17]). Thus, depending on the in-plane sizes of the rectangular magnetic element and the boundary conditions on its lateral edges, the quantized SW modes in the element could have frequencies that are either higher or lower than the frequency of the homogeneous ferromagnetic resonance in an infinite tangentially magnetized magnetic film.

Equation (8) also takes into account the fact that the considered rectangular magnetic element is nonellipsoidal, and the internal bias magnetic field in it is inhomogeneous. This inhomogeneity creates different effective internal magnetic fields $H_i^{mn}=\omega_H^{mn}/\gamma$ for different SW modes depending on their spatial distributions of variable magnetization, and, also, creates the integral form of wave vector quantization condition (5) along the direction of magnetization Oy.

COMPARISON WITH EXPERIMENT AND DISCUSSION

In order to use Eq. (7) in calculation of the spectrum of discrete SW modes measured for the square permalloy elements used in the spatially resolved ferromagnetic resonance experiments[18] we shall make an assumption about the lowest eigenmode distribution along the axis y. For the case of the experimental parameters as in Ref. 18 we have demonstrated above that the lowest $(n=0)$ quantized SW mode is localized in the center of the magnetic element, and the distribution of its amplitude along the axis y $\mu_0(y)$ should have a maximum at $y=0$. Thus, we shall choose a cosinusoidal function $\cos[(n+1)\pi y/l]$ with $n=0$ as a trial function for this mode distribution

$$\tilde{\mu}_0(y)=\cos(\pi y/l). \tag{12}$$

The function (12) reflects the most important features of the yet unknown *exact* magnetostatic eigenfunction $\mu_0(y)$. It is worth noting, that for the calculation of the resonance external bias fields corresponding to different quantized SW modes observed in the experiment[18] the exact shape of the function $\mu_0(y)$ is not very important due to small ratio of the thickness of the magnetic element to its in-plane sizes $(L/w=0.002)$.

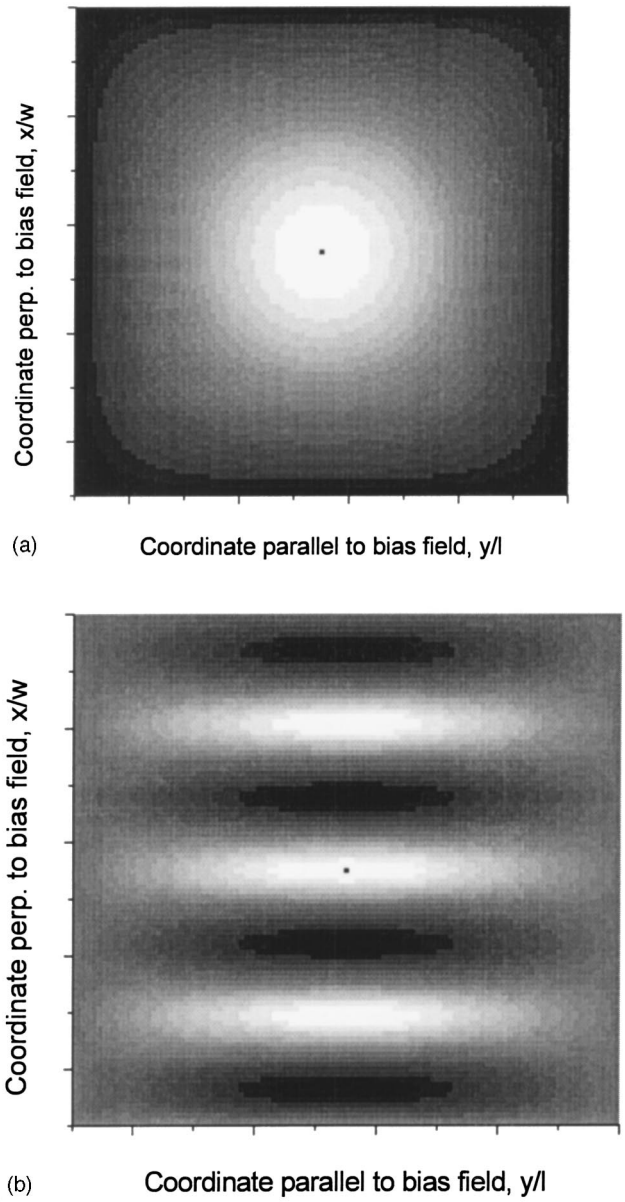

FIG. 5. Calculated dynamic magnetization distributions $m_{mn}(x,y)$ (contour plots) using Eq. (6) [see to compare with experiment the papers by Tamaru *et al.* (Ref. 18)]: (a) for the first SW mode $(m=0, n=0)$, (b) for the SW mode with $m=6$, $n=0$.

The nominal element thickness L of the magnetic element in Ref. 18 was 104 nm, while the width and length were equal to 50 μm. Refer back to exact form of the dependence $\mu_0(y)$ not being important [the correction to the trial eigenfunction (12) of order L/w will lead to the correction of order $(L/w)^2$ to the eigenfrequencies (7)]. A homogeneous bias magnetic field of the order of several hundred Oe was applied parallel to the side of the square. We assume that in such magnetic field the element is in the nearly uniform ''flower'' state. We would like to stress once more that the small aspect ratio $L/w(l=w)$ of the magnetic element allows us to use the approximate function (12) and the simple approximate dispersion equation (7) for the calculations of the SW spectrum of the square permalloy element.[18]

Using Eqs. (7)–(12) and assuming that eigenfrequencies for all the quantized SW modes experimentally observed in Ref. 18 are equal to the signal frequency $\omega_0/2\pi = 7.04$ GHz we calculated the values of the external bias field corresponding to the quantized SW modes.[18] The results of these calculations presented in the Table I demonstrate that the simple model equations (7)–(12) give a quantitative description of the experiment.[18]

The contour plots of two dimensional distribution of variable magnetization in quantized SW modes of the rectangular magnetic element[18] calculated using the approximate SW eigenfunctions (4), (12), and (6) are presented in Fig. 5 for the modes $(m=0, n=0)$ and $(m=6, n=0)$. Note that we used the SW eigenmodes, which are symmetric with respect to the rectangular element center. This corresponds to the SW excitation scheme by symmetric antenna in Ref. 18. The comparison of these distributions with the experimentally measured Kerr images of SW intensity in quantized SW modes observed in Ref. 18 (see Fig. 3, images P1 and P4, P5 in Ref. 18) demonstrates that our simple model gives a reasonably good qualitative description of the experiment.

CONCLUSIONS

We have shown that the quantized SW eigenmodes in a thin-film rectangular tangentially magnetized magnetic element can be calculated using a simple diagonal dispersion equation (7) that takes into account the quantiaztion of the in-plane components of the SW wave vector and the inhomogeneity of the internal bias magnetic field inside the element.

We have also shown that in the case of the magnetic element having relatively large in-plane sizes[18] the lowest SW modes are localized near the center of the element along the direction of static magnetization (axis Oy) and that this localization is of a purely dipolar nature in contrast with the case of a relatively narrow transversely magnetized magnetic stripe[10] where localization is of the exchange nature and takes place near the stripe lateral edges. The simple two-dimensional distributions of variable magnetization in quantized SW modes of a thin rectangular element found in this paper [see Eqs. (4), (12), and (6)] give good qualitative description of the experimental magnetization distributions measured in the experiment.[18]

ACKNOWLEDGMENTS

We would like to thank S. Tamaru and T. Crawford for presenting experimental details and G. Parker for useful discussion of demagnetizing field calculation. This work has been supported by the National Science Foundation (Grants No. DMR-0072017 and INT-0128823) and by the Oakland University Foundation.

[1] P. H. Bryant, J. F. Smyth, S. Schultz, and D. R. Fredkin, Phys. Rev. B **47**, 11255 (1993).
[2] C. Mathieu, J. Jorzick, A. Frank, S. O. Demokritov, A. N. Slavin, B. Hillebrands, B. Bartenlian, C. Chappert, D. Decanini, F. Rousseaux, and E. Cambril, Phys. Rev. Lett. **81**, 3968 (1998).
[3] J. Jorzick, S. O. Demokritov, C. Mathieu, B. Hillebrands, B. Bartenlian, C. Chappert, F. Rousseaux, and A. N. Slavin, Phys. Rev. B **60**, 15194 (1999).
[4] K. Yu. Guslienko *et al.* (unpublished).
[5] Y. Roussigne, S. M. Cherif, C. Dugautier, and P. Moch, Phys. Rev. B **63**, 134429 (2001).
[6] M. Grimsditch, Y. Jaccard, and I. K. Schuller, Phys. Rev. B **58**, 11539 (1998).
[7] S. O. Demokritov and B. Hillebrands, in *Spin Dynamics in Confined Magnetic Structures I*, edited by B. Hillebrands and K. Ounadjela (Springer, Berlin, 2002).
[8] E. Schloemann and R. I. Joseph, J. Appl. Phys. **35**, 167 (1964).
[9] T. Yukawa and K. Abe, J. Appl. Phys. **45**, 3146 (1974).
[10] J. Jorzick, S. O. Demokritov, B. Hillebrands, M. Bailleul, C. Fermon, K. Y. Guslienko, A. N. Slavin, D. V. Berkov, and N. L. Gorn, Phys. Rev. Lett. **88**, 047204 (2002).
[11] J. P. Park, P. Eames, D. M. Engebretson, J. Berezovsky, and P. A. Crowell, Phys. Rev. Lett. **89**, 277201 (2002).
[12] B. Hillebrands and J. Fassbender, Nature (London) **418**, 493 (2002).
[13] Th. Gerrits, H. A. M. van den Berg, J. Hohlfeld, L. Bar, and Th. Raising, Nature (London) **418**, 509 (2002).
[14] Y. Zhou, A. Roesler, and J. G. Zhu, J. Appl. Phys. **91**, 7276 (2002).
[15] N. Smith and P. Arnett, Appl. Phys. Lett. **78**, 1448 (2001).
[16] K. Yu. Guslienko, S. O. Demokritov, B. Hillebrands, and A. N. Slavin, Phys. Rev. B **66**, 132402 (2002).
[17] R. W. Damon and J. R. Eshbach, J. Phys. Chem. Solids **19**, 308 (1961).
[18] S. Tamaru, J. A. Bain, R. van de Veerdonk, T. M. Crawford, M. Covington, and M. H. Kryder, J. Appl. Phys. **91**, 8034 (2002); S. Tamaru *et al.* (unpublished).
[19] T. M. Crawford, M. Covington, and G. J. Parker, Phys. Rev. B **67**, 024411 (2003).
[20] B. A. Kalinikos and A. N. Slavin, J. Phys. C **19**, 7013 (1986).
[21] K. Yu. Guslienko and A. N. Slavin, J. Appl. Phys. **87**, 6337 (2000); J. Magn. Magn. Mater. **215–216**, 576 (2000).
[22] M. Sparks, Phys. Rev. B **1**, 3831 (1970).
[23] R. I. Joseph and E. Schlomann, J. Appl. Phys. **36**, 1579 (1965).
[24] A. Aharoni, J. Appl. Phys. **83**, 3432 (1998).
[25] S. O. Demokritov, B. Hillebrands, and A. N. Slavin, Phys. Rep. **348**, 441 (2001).
[26] C. Herring and C. Kittel, Phys. Rev. **81**, 869 (1951).